DALTON
PERSPECTIVE

Crystallography of molecular excited states. Transition-metal nitrosyl complexes and the study of transient species

Philip Coppens, Dmitry V. Fomitchev, Michael D. Carducci and Kirby Culp

Department of Chemistry, Natural Sciences and Mathematics Complex, State University of New York at Buffalo, Buffalo, New York 14260-3000, USA

The study of photoinduced processes in crystals is a frontier area of crystallographic research, which requires development of novel experimental and computational methods. In a series of studies, long-lived metastable states, generated upon photoirradiation of transition-metal nitrosyl complexes, have been identified as η^2 nitrosyl and isonitrosyl linkage isomers, and their detailed geometry has been determined. Calculations using density functional theory indicate that the species correspond to minima on the ground-state potential energy surface. The time-structure of synchrotron sources opens the possibility of time-resolved studies of transient species in crystals at the atomic level. Possible strategies for such experiments are described.

1 Introduction

Photochemical reactions in crystals have been an active area of research since the pioneering studies of Schmidt and coworkers,[1] who showed that the nature of the products of a solid-state reaction is topochemically-controlled by the geometry of the crystal structure. The work opened a new field of solid-state chemistry, typified by its close co-ordination of crystallographic and chemical methods.

Since that time, dramatic new technical developments in optical and X-ray technology have occurred. We now have at our disposal much more advanced instrumentation, including highly intense pulsed synchrotron sources, pulsed lasers, fiber optic light guides, cryostats, helium gas-flow systems and area detectors. At this point in time only our imagination limits the application of the new technologies. In combination, they offer the possibility of stroboscopic experiments on transient species with lifetimes of μs and less.[2]

As dynamic processes are central to chemistry, such studies will constitute a highly relevant extension of structure determination techniques, which until now have been essentially restricted to the elucidation of ground-state structures. How-

Philip Coppens received his Doctorate in Chemistry in 1960 from the University of Amsterdam with Professor Carolyn MacGillavry, based on work done at the Weizmann Institute of Science under the guidance of Professor Gerhard Schmidt. He has worked at Brookhaven National Laboratory, and at present carries the rank of Distinguished Professor of Chemistry at the State University of New York at Buffalo. His research interests include X-ray charge density analysis, chemical applications of synchrotron radiation crystallography and the study of photoinduced states in molecular crystals. He is a past President of the International Union of Crystallography.

Dmitry Fomitchev was born in 1968 in Moscow, Russia. He received his MS in Inorganic Chemistry in 1992 from the Moscow State University under the supervision of Professors Leonid M. Kovba and Eugene V. Antipov. Since 1994, he has been a graduate student at the State University of New York at Buffalo in the laboratory of Professor Philip Coppens where he is involved in the study of the light-induced metastable states of transition-metal nitrosyls. Inorganic chemistry is the major field of his research interests.

Michael Carducci, born in 1965 in California, received his Doctorate in Inorganic Chemistry during 1994 from the University of Arizona under the supervision of John Enemark and his Bachelors of Science from the University of California at Irvine working for Robert Doedens. Since 1995, he has been a postdoctoral associate at the State University of New York at Buffalo in the laboratory of Philip Coppens where he has studied photoinduced metastable species and time-resolved crystallography. His research interests extend throughout the fields of molecular and electronic structure determination.

Kirby Culp is finishing his undergraduate studies at the State University of New York at Buffalo. He has previously studied at SUNY Plattsburgh and the University of Maryland extension in Munich, Germany.

Philip Coppens

Dmitry Fomitchev

Michael Carducci

Kirby Culp

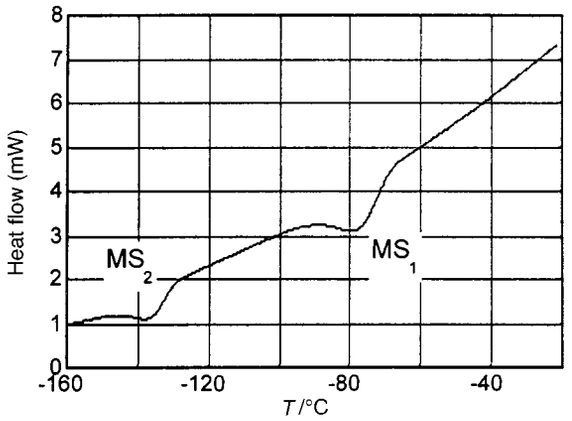

Fig. 1 Differential scanning calorimetry curve for a laser-irradiated crystal of sodium nitroprusside

ever, at present the use of X-ray diffraction in the analysis of metastable and transient species is still in its infancy.

Because the percentage of the molecules in a crystal that is excited depends on the beam intensity, the quantum efficiency, and the rate of the deactivation process, in general not all molecules in a crystal will be converted to the excited state. It is therefore necessary that approaches for analysis and interpretation of diffraction patterns of partially excited crystals be developed. Some such methods are illustrated below, and used in the diffraction analysis of novel configurations of transition-metal nitrosyl compounds. While the metastable states of the transition-metal nitrosyl complexes have been described in the literature as electronically excited states[3,4] with unusually long lifetimes at reduced temperatures, the crystallographic experiments lead to a different conclusion. A strategy for stroboscopic experiments on transient species, using the time-structure of synchrotron sources,[5] is discussed in the second part of this Perspective.

2 The Photochemistry of Nitrosyl Complexes

The photosensitivity of transition-metal nitrosyl compounds of iron was discovered in 1977 by Hauser *et al.*,[6] who studied optical dispersion changes in iron-containing photo-irradiated solids, using Mössbauer spectroscopy at low temperature. The prototype of the iron complexes is sodium nitroprusside (SNP), $Na_2[Fe(CN)_5NO]$, which in the solid state occurs as a dihydrate. The effect is not limited to solids, but also occurs in glassy matrices.[7] It was subsequently found that similar long-lived states can be generated by irradiation of nitrosyl complexes of Ru or Os,[8,9] with different ligands, different cations, and varying numbers of solvent molecules.

In the same year as the discovery by Hauser *et al.*, Crichton and Rest[10] reported changes in IR frequencies that occur on irradiation of cyclopentadienylnitrosylnickel [Ni(NO)(η^5-Cp)], in Ar, N_2, CO, and methane matrices at 20 K. According to the classification of Enemark and Feltham,[11] in which the d electrons are counted together with those electrons on the ligand which occupy σ^* or π^* levels, the ground state of the photosensitive nitrosyl complexes of Fe, Ru and Os is described as $\{M(NO)\}^6$, while [Ni(NO)(η^5-Cp)] and other complexes, such as $[Mn(CO)_4(NO)]$ and $[Mn(CO)(NO)_3]$, subsequently described by Crichton and Rest, have the $\{M(NO)\}^8$ or $\{M(NO)\}^{10}$ configurations.

Differential scanning calorimetry (Fig. 1) and low-temperature spectroscopic studies of SNP show that in addition to the first photoinduced state, MS_1, a second metastable state, labeled MS_2, exists. Infrared and Raman measurements show C–N, N–O, Fe–N stretching modes and the Fe–N–O bending mode to be downshifted on formation of the metastable states, the shifts for the modes associated with the M–N–O group

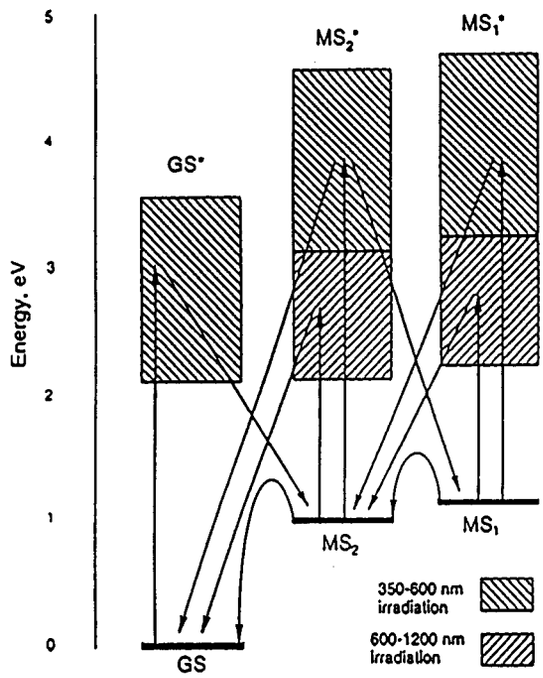

Fig. 2 Proposed relationship and interconversion pathways between the different states of SNP. Straight vertical arrows are electronic transitions. Slanted arrows combine an electronic transition with nuclear motion. Curved arrows are radiationless thermal decay (ref. 15)

being an order of magnitude larger than the small ($\approx$10 cm^{-1}) downshifts for the other vibrational frequencies.[12] The metastable states decay to the ground state at temperatures around 195 K (MS_1) and 151 K (MS_2) (Fig. 1). Thus, the MS_2 state can be eliminated by warming above 151 K, while an MS_1-free excited crystal can be obtained by converting the MS_1 state to MS_2 by irradiation with 1064 nm photons. The spectroscopic and thermal analyses indicate that the metastable states are not populated directly, but that population occurs through a transient higher energy state, and that at least some of the MS_1 species are formed through the MS_2 state as intermediate.[13,14] Various interconversion processes involving the ground and metastable, and corresponding excited states are illustrated in Fig. 2.

It has usually been assumed that the initial transition is an electronic excitation from the HOMO, $2b_2$ (d_{xy}) orbital to the LUMO, 7e (π^* NO) orbital (using the approximate C_{4v} point group symmetry),[16] leading to an excited complex which subsequently relaxes into two different metastable states,[17] though d–d transfer to a metal d_{z^2} orbital has also been proposed.[18] In any case, the states are not triplet states, as Mössbauer[19] and ESR[18] evidence indicate that both MS_1 and MS_2 are diamagnetic. It is also noteworthy that decay of the metastable states is radiationless.[20] In 1990 Güdel[21] pointed out that the longevity of the metastable states is inconsistent with any one-electron transfer model, and that either a large structural change, or a multi-electron promotion is required to explain the stability of the species.

The $\{M(NO)\}^{10}$ complexes appear to be stable only at much lower temperatures, but the postulated mechanism similarly involves photoelectron transfer to the NO^+ ligand. Far fewer studies have been reported on these complexes.

3 Photocrystallographic Experiments

In order to perform excited-state diffraction experiments, instrumentation and methods for such studies must be developed. The crystal must usually be kept at reduced temperatures, often below that of liquid N_2, and be simultaneously accessible to X-rays and the laser beam. In our equipment this is accomplished with a DISPLEX cryorefrigerator, mounted in the χ-circle of a Huber 512 diffractometer (Fig. 3). The optics

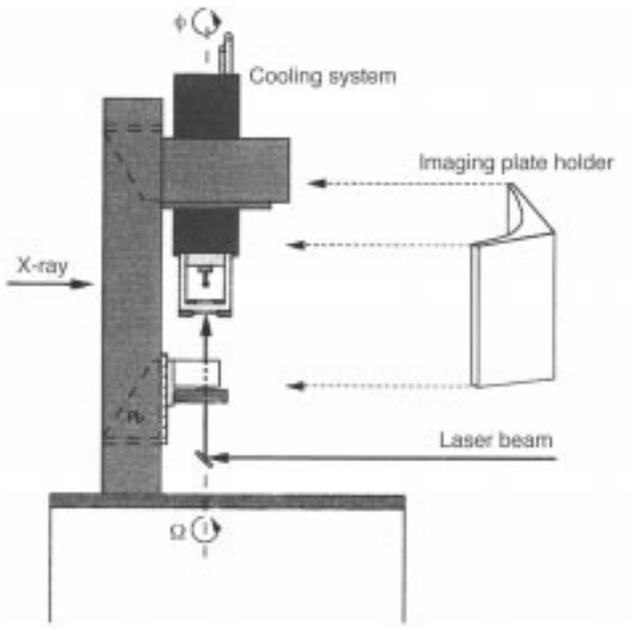

Fig. 3 Schematic drawing of the experimental arrangement used in the photocrystallography experiments

are attached to the edge of the χ-circle with a specially designed optical plate. When the oscillation method is used, a simple mirror system is adequate because the crystal rotation during data collection is limited to one axis. However, for conventional data collection with a point detector both the χ and ω diffractometer angles must be adjusted for each reflection, and flexible fiber optics and a lens system are needed.[22] The vacuum chamber (XTRANS, Anholt Technologies Inc.), which surrounds the crystal, is made of an X-ray transparent carbonaceous material,[23] with UV-transparent quartz optical windows mounted in its roof for access of the laser beam.

For long-lived species, such as the nitrosyl complexes described above, the irradiation period can preceed the entire X-ray exposure. For short-lived transient species, the X-ray and laser pulses must be synchronized to allow the probing of the sample during or just after excitation, when the population of the photoinduced species is at a maximum.[24] In both cases the experiment requires a comparison of the photoexcited and the ground-state crystal, both in reciprocal and real space. The reciprocal space comparison of reflection intensities is particularly important when conversion percentages are small, because a difference between two intensities measured in rapid succession can be measured to a better accuracy than the intensity itself. In the differential experiment, systematic effects with a longer time-scale, such as beam intensity or position variation, will not affect the results.

For a crystal in which only part of the molecules are excited, the structure factor expression, assuming random distribution of the excited molecules, and the presence of only two species, is given in equation (1) where the subscripts gs and es represent

$$F = (1 - P)F'_{gs} + PF_{es} + F_{rest} \quad (1)$$

the ground and metastable states respectively, P is the conversion percentage, and the subscript 'rest' represents inert moieties such as water of crystallization or counter ions not involved in the excitation. The term F'_{gs} may not be identical to F_{gs}, the structure factor of the ground-state crystal, as the ground-state molecules may move or rotate slightly due to the changed molecular environment. However, in studies we have done so far such effects appear minor, even when conversion percentages are close to 50%. We note that unit cell changes upon irradiation will also lead to slight differences between F'_{gs} and F_{gs}, and must therefore be taken into account. Simplifications may be introduced in the model, such as the assumption that the thermal parameters of the excited state are equal to those of the ground state. Especially when only a small fraction of the molecules are excited, such constraints may be essential to achieve convergence in the refinement.

Expression (1) allows the parametrization of the excited state molecule in terms of structural and charge density parameters, and therefore makes it possible to plot the charge density of the excited-state molecule.[25] Such detailed charge density experiments are only in the planning stage, but potentially allow identification of the electronic structure of an excited complex.

When conversion percentages are small, a better procedure is to analyze the *response ratio*, defined first in studies of the effect of an external electric field on the X-ray diffraction intensities.[26] The response ratio is given by expression (2) where I_{on} is based

$$\eta_{hkl} = \frac{I_{on}(hkl) - I_{off}(hkl)}{I_{off}(hkl)} = \frac{F^2_{on}(hkl) - F^2_{off}(hkl)}{F^2_{off}(hkl)} = \frac{F^2_{on}(hkl)}{F^2_{off}(hkl)} - 1 \quad (2)$$

on the structure factor as defined in (1), and I_{off} is related to the conventional ground-state structure factor expression. The response ratio thus gives the relative change of a reflection intensity as a result of the external perturbation. The parameters of the excited complex can be refined directly from the observed response ratios. The derivative expressions that are needed in the least-squares analysis of η are given in ref. 24.

4 Studies on Nitrosyl Complexes

4.1 Crystallographic studies and theoretical calculations

A first test of changes induced by photoirradiation is a difference map, in which the ground-state density is subtracted from the experimental density of the excited crystal. For centrosymmetric crystals, the calculated signs of the structure factors can be used with impunity, for acentric systems a phase error will be introduced, which may have to be considered. Sections of the Fourier-difference maps for centrosymmetric sodium nitroprusside, after the initial refinement of the rigid-body ground-state anion, for both MS_1 and MS_2 are shown in Fig. 4.[15] As the section in this figure contains two of the equatorial ligands, it is inclined by 45° to the crystallographic mirror plane that bisects the anion in the space group *Pnnm*. In both cases the iron atom is located on a pronounced slope in the δρ difference maps, flanked by a peak and a deep trough. This indicates that the atom has moved on irradiation in the direction of the peak position. It is interesting that in MS_1 the shift is *away* from the NO ligand, while in MS_2 the Fe is displaced *towards* this ligand, as indicated by the opposite slope of δρ at the Fe position in the two maps. On the other hand, the equatorial ligands are displaced *towards* and *away* from the nitrosyl group respectively, as indicated by peaks adjacent to the equatorial CN atoms. Some of the density remaining in the bonds is overlap density, not accounted for in the spherical atom formalism of this part of the analysis.

The remaining features of Fig. 4 are indicative of the nitrosyl groups. For MS_2 they appear near the ground-state N4 nitrogen position on both sides of the N–O bond. Corresponding minima at the ground-state N4 and O1 positions indicate a reorientation of the nitrosyl group atoms upon excitation.

In agreement with the difference map features, subsequent least-squares refinement of the MS_2 data leads to the sideways-bound η^2 geometry of NO shown in Fig. 5. It indicates a hitherto unknown species, with the NO group in an eclipsed, rather than the sterically less demanding staggered conformation. Since the NO group is located in a mirror plane in the ground-state crystal, two mirror-related eclipsed positions are

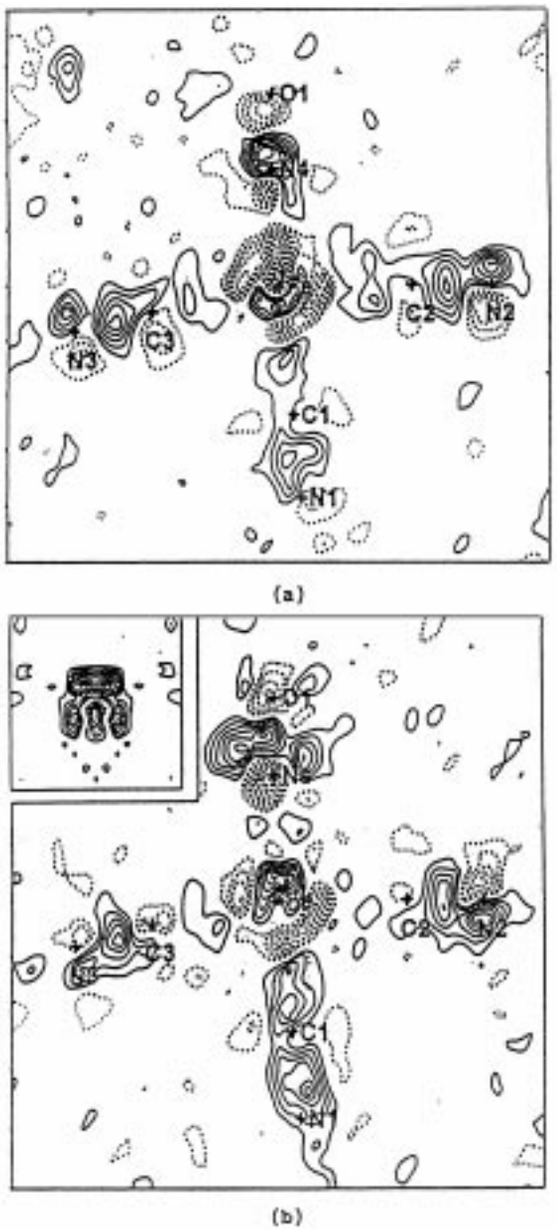

Fig. 4 Difference in electron density between the photoirradiated sodium nitroprusside crystal and ground-state molecules. Contours at 0.1 e $Å^{-3}$, zero contour omitted, negative contours broken. Crosses indicate the ground-state species atomic positions; (a) for the first metastable state MS_1, (b) for the second state MS_2. The insert shows a section perpendicular to the ground-state NO bond, chosen such as to contain the residual peaks (ref. 15)

Table 1 Isotropic 'thermal' mean-square displacements ($Å^2$), 50 K, for ground-state and MS_1 metastable state complexes, the latter both in the nitrosyl and isonitrosyl formulation

$Na_2[Fe(CN)_5(NO)]$ (ref. 15)

	Ground state	MS_1 Fe(NO)	MS_1 Fe(ON)
Proximal	0.0056(1)	0.0040(4)	0.088(5)
Distal	0.0116(1)	0.0163(5)	0.0102(4)

$K_2[Ru(OH)(NO)(NO_2)_4]$ (ref. 28)

	Ground state	MS_1 Ru(NO)	MS_1 Ru(ON)
Proximal	0.0072(5)	0.0037(13)	0.008(1)
Distal	0.0141(5)	0.022(2)	0.015(2)

$[Ru(Cl)(NO)(py)_4][PF_6]_2$ (ref. 29)

	Ground state	MS_1 Ru(NO)	MS_1 Ru(ON)
Proximal	0.0081(4)	0.0042(5)	0.0108(6)
	0.0128(5)	0.0061(5)	0.0175(7)
Distal	0.0135(4)	0.0232(7)	0.0117(6)
	0.0203(5)	0.0293(8)	0.0151(6)

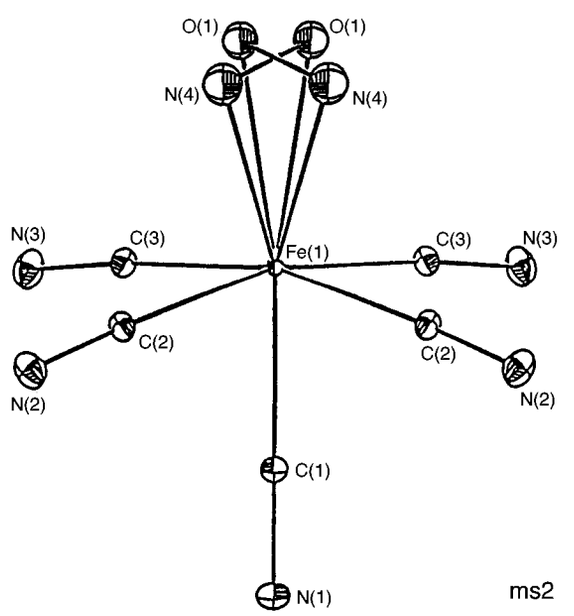

Fig. 5 An ORTEP[27] diagram of the MS_2 anion of sodium nitroprusside. Both mirror-related NO conformations are displayed, 50% probability ellipsoids are shown (ref. 15)

occupied after excitation. Clearly MS_2 is a linkage isomer rather than an electronically excited state.

Can MS_1 similarly be a linkage isomer? Geometric changes resulting from refinement of the MS_1 data are the lengthening of the Fe–(NO) distance by 0.053(6) Å, accompanied by an increase in the C(2)–Fe–C(3) angle by 1.1(3)° to 170.0(3)°, while the Fe–N–O angle and N–O bond length are not significantly changed from the ground-state values. A more pronounced change, however, occurs for the temperature parameters of the atoms of the NO ligand. Invariably, in this and other analogous studies we have performed (Table 1), the proximal atom has abnormally small values of the mean-square displacement parameters, while the distal atom shows excessively large values. It is well known, and has recently again been emphasized,[30] that assignment of an incorrect element-type to an atomic position leads to anomalous temperature parameters. In the present case, the anomaly is related to the observed decrease of density on the proximal, and increase of electron density on the distal atom, as described above. Since the *interchange* of the O and N atoms of the nitrosyl group removes the anomaly for SNP and for all other cases we have studied, the indication is that MS_1 is an isonitrosyl complex, in analogy with well known isocyanides. The disappearance of the anomaly is illustrated for the $[Ru(OH)(NO)(NO_2)_4]^{2-}$ anion in Fig. 6.[28] When the isonitrosyl configuration is introduced, the metastable state temperature parameters become normal, with a terminal/proximal ratio comparable to that of the ground state atoms, as shown in Table 1 for SNP, $K_2[Ru(OH)(NO)(NO_2)_4]$, and $[Ru(Cl)(NO)(py)_4][PF_6]_2$.[29] In all four cases (there are two independent molecules in the cell of the last complex), the ratio of the thermal parameters with the nitrosyl assignment of MS_1 is four or more, while it is quite normal for the isonitrosyl configuration. Evidence for the 'inverted' isonitrosyl configuration also comes from a neutron diffraction study. As nitrogen is a stronger neutron scatterer than oxygen, in this case the incorrect assumption leads to an anomalously *small* thermal parameter for the terminal atom. As expected, examination of peak heights in

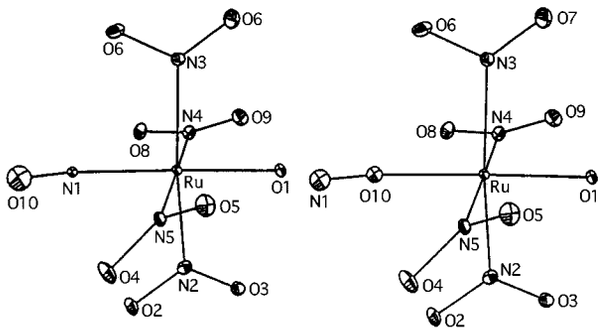

Fig. 6 The ORTEP drawings of the Ru–NO (left) and Ru–ON (right) models for the MS_1 excited state of the $[Ru(OH)(NO)(NO_2)_4]^{2-}$ anion, showing the differences in the nitrosyl thermal parameters. Thermal parameters for the other atoms are the same as those for the ground-state molecules, 50% probability ellipsoids are shown. The hydroxyl hydrogen atom has been omitted (ref. 28)

Fourier maps based on the X-ray data invariably gives corroborating information.

At this stage we concluded that both purportedly electronically excited states of the $\{M(NO)\}^6$ (Fe or Ru) nitrosyl complexes are linkage isomers, with MS_2 an intermediate on the pathway from the ground state to MS_1. We therefore decided to examine the $\{M(NO)\}^{10}$ complexes studied by Crichton and Rest. As $[Ni(NO)(\eta^5\text{-Cp})]$ is a liquid at room temperature, we synthesized and determined the structure of (pentamethylcyclopentadienyl)nitrosylnickel, $[Ni(NO)(\eta^5\text{-Cp*})]$.[31] In agreement with what was reported in EXAFS studies of $[Ni(NO)(\eta^5\text{-Cp})]$,[32] we find that photoexcitation to a long lifetime state requires very low temperatures, below about 60 K. Irradiation of a diffractometer-mounted single crystal of $[Ni(NO)(\eta^5\text{-Cp*})]$ with laser light (458 nm) at 25 K, produces the change in intensities and cell dimensions typical for photoexcitation in the solid state. There are two molecules in the asymmetric unit of the ground-state monoclinic $[Ni(NO)(\eta^5\text{-Cp*})]$ crystals, labelled here A and B, both with the NO axis oriented along the *b* axis of the unit cell. The observed shortening upon irradiation of the axis along which NO is oriented (from 14.355 to 14.078 Å)[31] is typical for formation of an MS_2-type species, and also observed for SNP, though in that case the NO axis is not perfectly aligned with the crystallographic axes. When an MS_1 species is formed, on the other hand, the corresponding cell dimension will lengthen, reflecting the increased distance from the metal to the proximal atom of the NO ligand. The formation of an MS_2 species is confirmed by the photodifference map, shown in Fig. 7, which very clearly indicates the depletion of density along the axial direction, and the build-up in off-axis regions. Subsequent analysis shows that the NO group of the second molecule has two different orientations, both approximately parallel to the Cp* ring. The conversion percentage achieved in this experiment, as obtained in the least-squares analysis, is much higher than that for SNP, 47% *vs*. 9.5%. The difference is likely due to the experimental conditions, specifically the necessity, in the case of SNP, to eliminate MS_1 by subsequent irradiation with light of 1064 nm.

The high conversion percentage allows a reasonably accurate determination of the geometry of the excited $[Ni(NO)(\eta^5\text{-Cp*})]$ species (Fig. 8). Bond lengths of the nitrosyl ligand and those involving the Ni atom are listed in Table 2. The average metastable state Ni–O distance is 2.087 Å, the Ni–N distance is lengthened by about 0.09 Å, and there is an increase of about 0.02 Å in the distance from the Ni atom to the Cp* plane. As in SNP, no significant change occurs in the NO distance. The latter is surprising and unexplained, given the large decrease of 446 cm^{-1} in the IR stretching frequency of NO. For comparison, the EXAFS studies led to the conclusion that the Ni–N bond was elongated by 0.12(3) Å, and the Ni–N–O angle

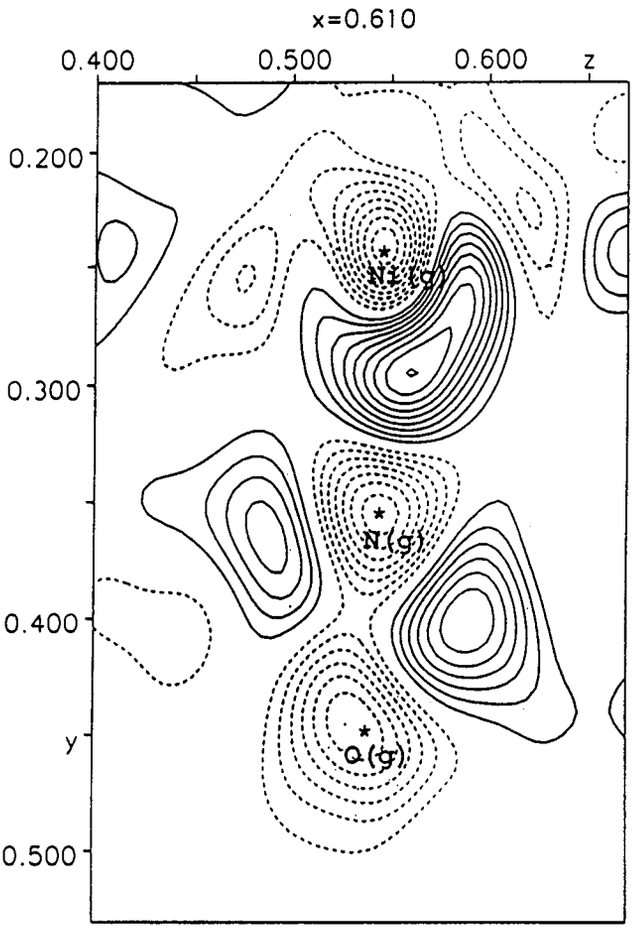

Fig. 7 Difference in electron density between the photoirradiated $[Ni(NO)(\eta^5\text{-Cp*})]$ crystal and ground-state molecules. Contours at 0.4 e $Å^{-3}$. Negative contours dotted (ref. 31)

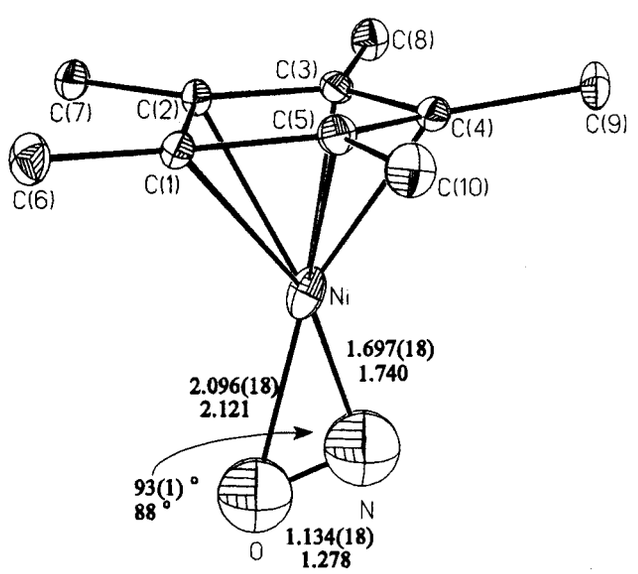

Fig. 8 The geometry of the photogenerated $[Ni(\eta^2\text{-NO})(\eta^5\text{-Cp*})]$ species (based on ref. 31). Some of the interatomic distances and angles are indicated. Top line: experimental values, lower line from theoretical optimization with the B3LYP functional and the LANL2DZ basis set

bent from 180° to 160° or even 133°. While the lengthening of the Ni–N bond is confirmed by the crystallographic structure determination, the bending is more pronounced than inferred from the EXAFS study.

Additional support for the existence of the linkage isomers comes from theoretical calculations, which confirm that the

Table 2 Selected bond lengths (Å) for ground and metastable state structures of the [Ni(NO)(η^5-Cp*)] at 25 K (ref. 31)

	Ground state		Metastable state	
Bond	Molecule A	Molecule B	Molecule A	Molecule B
Ni–N	1.620(3)	1.614(3)	1.697(18)	1.724(10)/ 1.716(10)
Ni–O			2.096(18)	2.077(10)/ 2.079(10)
Ni–plane[a]	1.719(1)	1.718(1)	1.732(6)	1.750(6)
Ni–C(1)	2.107(3)	2.110(3)	2.092(12)	2.138(12)
Ni–C(2)	2.106(3)	2.110(3)	2.132(12)	2.132(11)
Ni–C(3)	2.109(3)	2.108(3)	2.142(11)	2.137(12)
Ni–C(4)	2.106(3)	2.104(4)	2.142(12)	2.120(12)
Ni–C(5)	2.105(3)	2.110(3)	2.106(12)	2.165(12)
N–O	1.177(3)	1.181(4)	1.134(18)	1.126(30)/ 1.128(32)

[a] The mean plane through the C(1), C(2), C(3), C(4), C(5) atoms of the Cp* ring.

Table 3 Calculated (B3LYP functional–LANL2DZ basis set) and experimental values for some of the bond lengths (Å) and angles (°) for the metastable structure of [Ni(η^2-NO)(η^5-Cp*)]. The experimental values for molecule A are listed (ref. 31)

	Theoretical	Experimental
Ni–C(1)	2.117	2.092(12)
Ni–C(2)	2.200	2.132(12)
Ni–C(5)		2.106(12)
Ni–C(3)	2.236	2.142(11)
Ni–C(4)		2.142(12)
Ni–N	1.740	1.697(18)
Ni–O	2.121	2.096(18)
N–O	1.278	1.134(18)
Ni–N–O	87.9	93(1)

Table 4 Relative energies (eV[a]) of the ground MS_1 and MS_2 states from theoretical calculations

	Ground state	MS_2	MS_1
SNP Theory	0	1.368(1.465)[b]	1.677(1.639)[b]
Experimental (ref. 20)	0	1.0	1.1
[Ni(NO)(η^5-Cp*)] Theory (ref. 31)	0	0.993	1.847

[a] eV ≈ 1.602×10^{-19} J. [b] Numbers in brackets refer to solid state calculations.

observed structures correspond to local minima on the ground-state potential energy surface. For SNP this is shown by an extended-Hückel based Walsh diagram of the end-to-end interconversion of the nitrosyl and isonitrosyl configurations, and more accurately, by a DFT calculation of Delley *et al.*[33] The DFT calculation correctly predicts the lower energy of the MS_2 configuration compared with MS_1, which is observed experimentally. For [Ni(NO)(η^5-Cp*)] we have performed a complete DFT geometry optimization of three different species: the ground state, the observed [Ni(η^2-NO)(η^5-Cp*)] metastable state and a hypothetical [Ni(ON)(η^5-Cp*)] isonitrosyl configuration. The theoretical geometry of [Ni(η^2-NO)(η^5-Cp*)] agrees rather well with the observed values (Table 3, Fig. 8), except for the NO bond, which is calculated to be considerably lengthened compared with the ground state, by an amount equal to 0.064 Å. For SNP, the lengthening of the NO bond is predicted to be much smaller according to the DFT calculation: 0.031 Å for MS_2 and a small shortening of 0.006 Å for MS_1. For MS_2 this difference correlates with the downshift of the NO stretching frequency, which is 284 cm^{-1} for SNP, compared with 446 cm^{-1} for [Ni(η^2-NO)(η^5-Cp)]. It is noteworthy that, notwithstanding the shortening of the NO bond in MS_1 of SNP, the calculation predicts a small decrease of the NO stretching frequency.

Table 5 Transition temperatures and conversion percentages reached for several transition-metal nitrosyl complexes

	T_c[a]/°C		Conversion (%) (may not be maximal[b])	
Compound	MS_1	MS_2		Ref.
$Na_2[Fe(CN)_5(NO)]$	−78	−122	48/≈30	37
$K_2[Ru(OH)(NO)(NO_2)_4]$	−65	−100	≈16/1	28
$[Ru(Cl)(NO)(py)_4][PF_6]_2$	−17.2	−102 (weak)	30 (MS_1)	29
$[Ru(Cl)(NO)(bipy)_2][PF_6]_2$	no	no	–	29
$[Ru(OH)(N_3)(NO)(py)_3][PF_6]$	−38.4	no	12	29
$[Ru(NO)(N_3)_3(py)_2]$	no	no	–	29
$[Ru(NH_3)_5(NO)]Cl_3$	0	no	≈2	29
Ni(NO)(η^5-Cp*)]	no	−240 to −200	47	31
trans-$[Ru(Cl)(en)_2(NO)]Cl_2$	−27	no	≈5	36
cis-$[Ru(Cl)(en)_2(NO)]Cl_2$	−67	no		36
trans-$[Ru(Br)(en)_2(NO)]Br_2$	−44	no		36
cis-$[Ru(Br)(en)_2(NO)]Br_2$	−62	no		36
trans-$[Ru(H_2O)(en)_2(NO)]Cl_3$	−6	no		36
$[Ru(Cl)_3(en)(NO)]$ (mixture of *fac* and *mer* isomers)	−68	no		36

[a] no Indicates that no metastable state has been observed. [b] First value MS_1, second value MS_2. Only one value is given if only one metastable state is observed.

The energy differences that are predicted are of the same order of magnitude as those deduced from the thermodynamic and spectroscopic measurements (Table 4), in both cases MS_2 is found to be the more stable linkage isomer, but the destabilization of MS_1 relative to MS_2 is much more pronounced for [Ni(NO)(η^5-Cp*)]. The fact that MS_1 has not been observed for the Ni complex, either crystallographically or spectroscopically, may be related to a correspondingly smaller barrier to deactivation for this species.

4.2 Solid-state photosensitivity of other nitrosyl complexes

Nitrosyl complexes such as SNP have been proposed as molecular storage devices in which information can be optically written, read and erased.[34] The dependence of the thermal depopulation temperature on chemical substitution is therefore of particular interest, as species stable at room temperature would be most attractive for applications. Variation of the cation in the nitroprusside salt series leads to only small variations in the transition temperature, which varies from 186 K for the tetramethylammonium salt to 218 K for $K_2[Fe(CN)_5NO]\cdot 2.5H_2O$.[35] However, we have found that chemical substitution in the complex cation of the Ru series leads to considerable variation in the deactivation temperature. The first metastable state (MS_1) of $[Ru(Cl)(NO)(py)_4][PF_6]_2$, for example, only decays at 256 K (−17.2 °C), while even higher decay temperatures have been observed for *trans*-$[Ru(H_2O)(en)_2NO]Cl_3$ and $[Ru(NH_3)_5(NO)]Cl_3$, though conversion percentages appear small in these cases. A summary of our results and those reported by Morioka and co-workers[36] is given in Table 5. The limited amount of data perhaps indicates that cationic complexes in general have higher decay temperatures. There are unexplained variations, such as the difference in behaviour upon substitution of two bipyridyl ligands for the four pyridines of the $[Ru(Cl)(NO)(py)_4]^{2+}$ cation (third and fourth entries in Table 5). It is possible that the crystalline environment plays a role in determining the stability of the metastable states. Photoinduced deactivation is also likely to differ from complex to complex. It is clear that additional experimental and theoretical work is needed before the factors influencing the relative stability of the metastable nitrosyl complexes can be understood.

5 Perspectives for the Study of Transient Species

5.1 Time-resolved experiments using pulsed synchrotron sources

Many species of interest in chemistry have lifetimes of μs, ns or shorter. There are also a great many fast processes, such as electron transfer within and between molecules, which are of crucial importance in chemistry and biology. To study such processes, the use of non-steady state methods becomes imperative. Rather than establish a steady-state concentration by relatively long laser irradiation, an instantaneous non-equilibrium concentration is established and probed before significant decay occurs. Such experiments have now been performed to study processes like the photodissociation and recombination of myoglobin and carbon monoxide.[38,39] In these experiments the polychromatic Laue technique is used with a single synchrotron bunch of 60 ps length. By varying the delay between the exciting pump pulse and the probe pulse, the reversible dynamic process can be followed on a very fine time-scale, and a 'motion picture' of the reaction can be obtained.

For experiments that aim at detailed atomic and even electronic resolution, monochromatic methods promise better accuracy. To perform the experiments in a reasonable time span, parallel, rather than sequential reflection measurement techniques must be used. Electronic detectors, such as CCD's now have read-out times of a few seconds, and allow a rapid succession of light-on and light-off measurements at each angular oscillation range of the crystal.

For such experiments to be successful, the number of photons in the exciting laser pulse must be of the same order of magnitude as the number of molecules in the crystal. This is well within reach of current technology. A 5 kHz Nd-YAG laser with a 50 mJ pulse energy gives, for example, about 10^{14} photons per pulse at 355 nm. For a typical complex, the number of 10^{14} molecules corresponds to a $40 \times 40 \times 40$ μ crystal, which is what is used in many synchrotron diffraction experiments. Working with small sample crystals has the further advantage that illumination is more uniform, and heat dissipation to the surroundings is enhanced. A reasonably uniform illumination requires that only a fraction of the incident beam is absorbed, so that not all photons will lead to excitation. To counter this effect, the number of active molecules can be reduced further by embedding the molecules as hosts in a spectroscopically inert matrix.

Thus, the active molecule–photon ratio and the transparency requirement all indicate that very small samples must be used, which means that experiments are most likely to be successful at the brightest synchrotron sources.

At the Advanced Photon Source at Argonne National Laboratory, where our experiments are to be carried out, the orbit flight time is 3.68 μs, or a frequency of about 0.27 MHz. This means that only a small fraction of the X-ray pulses can be used in the experiment, a not so serious limitation given the brightness of the sources available, but nevertheless a factor that will limit the possibilities for use of even smaller samples. An X-ray free electron laser with its much lower repeat rate may eventually be the optimal source for stroboscopic laser-triggered experiments! For the synchrotron source, the need to eliminate a large fraction of the X-ray pulses adds an additional level of complexity, as it dictates the use of a very fast shutter or pulse selector. Several designs for such devices are now being developed. A detector with very fast read-out capability, now being tested,[40] may offer an alternative to the fast shutter, and produce a concomitant simplification of the experimental set-up. A schematic description of the experiment is given in Fig. 9.

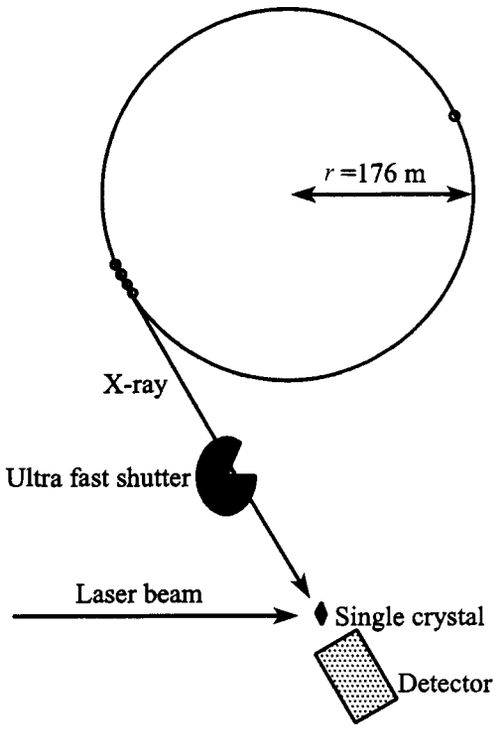

Fig. 9 Schematic of the time-resolved synchrotron experiment (numerical information based on the Advanced Photon Source parameters). The electron bunches travel around the storage ring with a flight time of 3.68 μ, and produce flashes of X-rays incident on the sample crystal. Either a single bunch, or a 'superbunch' consisting of multiple bunches may be used

5.2 What systems can be studied?

Though the relevance of time-resolved studies is expected to be very extensive, and involve a variety of chemical processes, we will, for illustration, give a few examples of possible applications.

(a) Transition-metal complexes. Many transition-metal complexes have excited triplet states with long lifetimes. Prime examples are complexes of rhodium studied more than twenty years ago by Crosby and co-workers.[41] The light-induced triplet state of $[RhBr_2(C_5D_5N)_4]Br$, for instance, has a lifetime of 1.5 μs in the solid state. With such long lifetimes, even conventional sources offer some possibilities, as we have recently demonstrated in a series of test experiments in preparation for the synchrotron studies.[24] In these experiments a steady-state concentration of excited molecules was maintained during a period of about 20 ms. In the synchrotron experiments, on the other hand, no equilibrium is to be established, and a much shorter lifetime species can be studied.

Examples of transition-metal complexes with photoinduced excited triplet states having μs lifetimes are the binuclear metal d^8–d^8 complexes of rhodium and platinum. They show unusual reactivity, and are, in solution, intermediates in metal-catalyzed photoreactions of small molecules and organic substrates.[42] Since for these d^8–d^8 complexes the excitation corresponds to a $d\sigma^* \longrightarrow p\sigma$ transition, very large contractions of the metal–metal distance occur if the bridging ligands are sufficiently flexible. An example is $Rh_2(dimen)_4^{2+}$ (dimen = 1,8-diisocyanomenthane) for which metal–metal bond shortening from 4.8 Å to 3.2 Å upon excitation to a 21 μs lifetime state has been deduced from spectroscopic information. On the other hand, single metal–metal bond $Rh^0{}_2$ and Rh^0Rh^{II} complexes with the bridging ligand bis(difluorophosphine)methylamine, $(PF_2)CH_3N(PF_2)$, undergo excitation into a $d\sigma^*$ orbital, and are expected to show bond lengthening upon excitation.[43] As illustrated above for the transition-metal nitrosyl complexes, the diffraction experiment is capable of yielding the full three-dimensional structure of the photoinduced state. At present such information is completely lacking for shorter lived species.

(b) Photoinduced electron transfer and charge-separated states. An intriguing field for time-resolved studies is photoinduced electron transfer. For such studies, the time resolution

may need to be increased to nanoseconds or better. Factors limiting time resolution in the techniques described above are jitter in the laser pulses and the width of the probing X-ray pulse, which is of the order of 100 ps. However, other experimental arrangements have been proposed.[44] Possible candidates are triad molecules, containing, for instance, a carotenoid donor, porphyrin or metal–porphyrin bridge and quinone acceptor(s).[45] We note that such molecules have been studied extensively because of their relevance for energy conversion and the storage of information,[46,47] and that they have been proposed as components of molecular computing devices.[48] Information on geometry changes along the reaction path of the photochemical charge separation and recombination would shed new light on the mechanism of electron transfer and of photoinduced processes in chemical and biologically important systems.

6 Concluding remarks

We may expect that within the next decade time-resolved experiments will become widespread, thus opening a novel field of diffraction studies of broad relevance to chemistry. Such experiments may yield presently not accessible information at the atomic level and beyond, on processes that are at the center of current interest. The results on the metastable isomers of transition-metal nitrosyl complexes, described above, have revealed the existence of previously unknown species, and in addition allowed the development of methods to be used in future studies of transient states.

7 Acknowledgements

Support of this work by the National Science Foundation (CHE9615586) and the Petroleum Research Fund administered by the American Chemical Society (PRF28664AC3) is gratefully acknowledged. Figs. 2 and 4–8 were reproduced with permission from the American Chemical Society.

8 References

1 M. D. Cohen and G. M. J. Schmidt, *J. Chem. Soc.*, 1964, 1996; M. D. Cohen, *Angew. Chem.*, 1975, **14**, 386.
2 P. Coppens, *Synchrotron Radiat. News*, 1997, **10**, 26.
3 M. Rüdlinger, J. Schefer, G. Chevrier, N. Furer, H. U. Güdel, S. Haussühl, G. Heger, P. Schweiss, T. Vogt, Th. Woike and H. Zöllner, *Z. Phys. B*, 1991, **83**, 125.
4 J. A. Güida, O. E. Piro, P. S. Schaiquevich and P. J. Aymonino, *Solid State Commun.*, 1997, **101**, 471.
5 D. M. Mills, *Rev. Sci. Instrum.*, 1989, **60**, 2338; D. M. Mills, *Handb. Synchrotron Radiat.*, 1991, **3**, 291.
6 U. Hauser, V. Oestreich and H. D. Rohrweck, *Z. Phys. A*, 1977, **280**, 17; 1977, **280**, 125; 1978, **284**, 9.
7 H. Zöllner, W. Krasser, Th. Woike and S. Haussühl, *Chem. Phys. Lett.*, 1989, **161**, 497.
8 Th. Woike and S. Haussühl, *Solid State Commun.*, 1993, **86**, 333; J. A. Guida, O. E. Piro and P. J. Aymonino, *Inorg. Chem.*, 1995, **34**, 4113.
9 L. M. Baraldo, M. S. Bessega, G. E. Rigotti and J. A. Olabe, *Inorg. Chem.*, 1994, **33**, 5890.
10 O. Crichton and A. J. Rest, *J. Chem. Soc.*, *Dalton Trans.*, 1977, 986; 1978, 202; 1978, 208.
11 J. H. Enemark and R. D. Feltham, *Coord. Chem. Rev.*, 1974, **13**, 339.
12 J. A. Güida, P. J. Aymonino, O. E. Piro and E. E. Castellano, *Spectrochim. Acta*, *Part A*, 1993, **49**, 535.
13 Th. Woike, W. Kirchner, G. Schetter, Th. Barthel, H. Kim and S. Haussühl, *Opt. Commun.*, 1994, **106**, 6.
14 Th. Woike, W. Krasser, H. Zöllner, W. Kirchner and S. Haussühl, *Z. Phys. D*, 1993, **25**, 351.
15 M. D. Carducci, M. R. Pressprich and P. Coppens, *J. Am. Chem. Soc.*, 1997, **119**, 2669.
16 Th. Woike, W. Krasser, P. S. Bechthold and S. Haussühl, *Solid State Commun.*, 1983, **45**, 499; *Phys. Rev. Lett.*, 1984, **53**, 1767.
17 Th. Woike, W. Krasser, H. Zöllner, W. Kirchner and S. Haussühl, *Z. Phys. D*, 1993, **25**, 351.
18 C. Terrile, O. R. Nascimento, I. J. Moraes, E. E. Castellano, O. E. Piro, J. A. Güida and P. J. Aymonino, *Solid State Commun.*, 1990, **73**, 481.
19 Th. Woike, W. Kirchner, H. Kim, S. Haussühl, V. Rusanov, V. Angelov, S. Ormandjiev, Ts. Bonchev and A. N. F. Schroeder, *Hyperfine Interact.*, 1993, **7**, 265.
20 H. Zöllner, Th. Woike, W. Krasser and S. Haussühl, *Z. Kristallogr.*, 1989, **188**, 139.
21 H. U. Güdel, *Chem. Phys. Lett.*, 1990, **175**, 262.
22 M. A. White, M. R. Pressprich. P. Coppens and D. D. Coppens, *J. Appl. Crystallogr.*, 1994, **27**, 727.
23 D. D. Coppens, P. Coppens, P. Lee and R. Li, *J. Appl. Crystallogr.*, 1993, **26**, 226.
24 Y. Ozawa, M. R. Pressprich and P. Coppens, *J. Appl. Crystallogr.*, in the press.
25 M. R. Pressprich, M. A. White, Y. Vekhter and P. Coppens, *J. Am. Chem. Soc.*, 1994, **116**, 5233; P. Coppens, *X-ray Charge Densities and Chemical Bonding*, Oxford University Press, IUCr, New York, 1997.
26 A. Paturle, H. Graafsma, H.-S. Sheu, P. Coppens and P. Becker, *Phys. Rev. B*, 1991, **43**, 683; H. Graafsma, P. Coppens, J. Majewski and D. Cahen, *J. Solid State Chem.*, 1993, **105**, 520.
27 C. K. Johnson, ORTEP, Report ORNL-5138, Oak Ridge National Laboratory, Oak Ridge, TN, 1976.
28 D. V. Fomitchev and P. Coppens, *Inorg. Chem.*, 1996, **35**, 7021.
29 D. V. Fomitchev, K. Culp and P. Coppens, unpublished work.
30 R. L. Harlow, *J. Res. Nat. Inst. Stand. Technol.*, 1996, **101**, 327.
31 D. V. Fomitchev, T. R. Furlani and P. Coppens, *Inorg. Chem.*, in the press.
32 X. L. Chen, M. K. Bowman, Z. Wang, P. A. Montano and J. R. Norris, *J. Phys. Chem.*, 1994, **98**, 9457.
33 B. Delley, J. Scheffer and Th. Woike, *J. Chem. Phys.*, 1997, **107**, 10 067.
34 Th. Woike, W. Kirchner, G. Schetter, Th. Barthel, H. Kim and S. Haussühl, *Opt. Commun.*, 1994, **106**, 6.
35 H. Zöllner, W. Krasser, Th. Woike and S. Haussühl, *Chem. Phys. Lett.*, 1989, **161**, 497.
36 K. Ookubo, Y. Morioka, H. Tomizawa and E. Miki, *J. Mol. Struct.*, 1996, **379**, 241.
37 J. Schefer, Th. Woike, S. Haussühl and M. T. Fernandez Diaz, *Z. Kristallogr.*, 1997, **212**, 29.
38 Z. Ng, K. Ren, G. E. O. Borgstahl, E. D. Getzoff and K. Moffat, *J. Appl. Crystallogr.*, 1996, **29**, 246; D. Bourgeois, T. Ursby, M. Wulff, C. Pradervand, A. Legrand, W. Schilkamp, S. Laboure, V. Srajer, T. Y. Teng, M. Roth and K. Moffat, *J. Synchrotron Radiat.*, 1996, **3**, 65.
39 U. K. Genick, G. E. O. Borgstahl, Z. Ng, K. Ren, C. Pradervand, P. M. Burke, V. Srajer, T. Y. Teng, W. Schilkamp, D. E. Mcree, K. Moffat and E. D. Getzoff, *Science*, 1997, **275**, 1471; V. Srajer, T. Y. Teng, T. Ursby, C. Prendervand, Z. Ren, S. Adachi, W. Schildkamp, D. Bourgeois, M. Wulff and K. Moffat, *Science*, 1996, **274**, 1726.
40 Y. Ohashi and H. Uekusa, *J. Mol. Struct.*, 1996, **374**, 37; T. Tanimori, A. Ochi, S. Minami and T. Nagase, *Nucl. Instrum. Methods in Phys. Res.*, *Sect. A*, 1996, **381**, 280.
41 D. H. W. Carstens and G. A. Crosby, *J. Mol. Spectrosc.*, 1970, **34**, 113; T. R. Thomas, R. J. Watts and G. A. Crosby, *J. Chem. Phys.*, 1973, **59**, 2123.
42 D. M. Roundhill, H. B. Gray and C.-M. Che, *Acc. Chem. Res.*, 1989, **22**, 55; D. G. Nocera, *Acc. Chem. Res.*, 1995, **28**, 209.
43 J. I. Dulebohn, D. L. Ward and D. G. Nocera, *J. Am. Chem. Soc.*, 1990, **112**, 2969.
44 R. Neutze and J. Hajdu, *Proc. Natl. Acad. Sci. USA*, 1997, **94**, 5651.
45 K. Hasharoni, H. Levanon, J. Tang, M. K. Bowman, J. R. Norris, D. Gust, T. A. Moore and A. L. Moore, *J. Am. Chem. Soc.*, 1990, **112**, 6477; J.-P. Collin, A. Harriman, V. Heitz, F. Odobel and J.-P. Sauvage, *J. Am. Chem. Soc.*, 1994, **116**, 5679, and refs. therein.
46 J. Mattay, *Top. Curr. Chem.*, 1989, 156.
47 C. A. Mirkin and M. A. Ratner, *Annu. Rev. Phys. Chem.*, 1992, **43**, 719.
48 J. J. Hopfield, J. N. Onuchic and D. N. Beratan, *Science*, 1988, **241**, 817; J. J. Hopfield, J. N. Onuchic and D. N. Beratan, *J. Phys. Chem.*, 1989, **93**, 6350.

Received 28*th November* 1997; *Paper* 7/08604K